VULNERABILITY ASSESSMENT OF THE S. JOÃO DE LOURE BRIDGE – VOUGA'S RIVER

Catarina A. L. Fernandes[1]; Humberto Varum[2]

Civil Engineering Department, University of Aveiro, 3810-193 Aveiro - Portugal
[1] cfernandes@civil.ua.pt [2] hvarum@civil.ua.pt

ABSTRACT

Steel bridges are particularly sensible to corrosion, which can put at risk the structural safety by affecting the joint elements. Having this in mind, the objective of this work was to evaluate the influence of the joint's stiffness in the structural response of the S. João de Loure steel bridge. An improved model was developed for the bridge on the structural analysis software SAP2000. Maximum deflection, axial forces and corresponding stresses, and natural frequencies, were analyzed. Numerical results allow concluding about the influence of the joint's stiffness in the structural response of the bridge.

1. GENERAL DESCRIPTION

The S. João de Loure bridge (Fig.1) is located in EN 230-2, km 0.601, S. João de Loure, Albergaria-a-Velha, district of Aveiro. It is a single span steel bridge and its main girders have 6 m spacing, are 4.35 m high and divided in eleven panels with 3.54 m length (Freire, Martins and Torres 1998). The main structure is supported by the masonry abutments: fixed supports in the north abutment and roller bearings in the south one. Examples of the joint elements are shown in Fig. 2. Table 1 summarizes the main geometrical characteristics of the bridge and the steel properties adopted in the numerical analysis.

Fig. 1. General views of the S. João de Loure bridge (Fernandes and Silva 2004).

(a) (b) (c)

Fig. 2. Joint elements: (a) Stringer / cross-girder; (b) Stringer / main girder; (c) Posts (Fernandes and Silva 2004).

Table 1 – Geometrical characteristics of the structure and steel properties

Main geometrical characteristics	
Number of spans	1
Span length	43.36 m
Steel deck length	44.00 m
Road width	4.40 m
Footways width	2×0.80 m
Bridge girders spacing	6.00 m

Steel properties	
Characteristic yielding stress f_{yk}	225 MPa
Characteristic ultimate stress f_{uk}	245 MPa
Young's modulus E	200 GPa

2. INFLUENCE OF THE JOINT'S STIFFNESS IN THE STRUCTURAL RESPONSE

2.1 Structural model, loads and combinations

The structural model introduced in this paper is an improvement of a model developed previously by Furtado and Marques (2003). In the original model, almost all nodes were considered hinged. In the improved model, the flanges were considered continuous elements. Furthermore, the diagonals and posts were divided in 3 sub-elements (Varum 2003; Fernandes and Silva 2004). Each bar element of length L was divided in a central element with length L' and lateral elements (length L_l), as represented in Fig. 3. The length of the lateral sub-elements, L_l, represents the joint's length in the corresponding elements and its value was established from the available drawings (S. João de Loure bridge – Drawings 2001).The posts were divided in 4 sub-elements. An additional node in the central sub-element was necessary to apply the loads from the cross-girder.

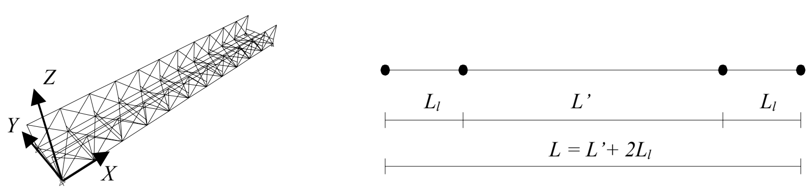

(a) (b)

Fig. 3. Structural model: (a) FE Mesh; (b) Improved model: consideration of 3 sub-elements.

The geometrical characteristics of the element's cross-section were calculated from the AutoCAD drawings (S. João de Loure bridge – Drawings 2001) and was made automatically with the numerical tools available (Table 2). The coordinate axes used for each cross-section were considered in the left inferior point. All bars have a uniform cross-section along its length.

The nomenclature adopted for the flanges, diagonals and posts in the structural analysis software (SAP2000 2003) is summarized in Fig. 4.

Table 2 – Geometrical characteristics of the element's cross-sections

	Label	Área	Center of Gravity		Moment of Inertia	
		A (m^2)	z_G (m)	y_G (m)	I_{zG} (cm^4)	I_{yG} (cm^4)
Flanges	*FL 1*	0.015870	0.1183	0.2250	9489	36987
	FL 2	0.020820	0.0999	0.2250	17842	42779
	FL 3	0.025770	0.0907	0.2250	26196	47228
	FL 4	0.025770	0.0862	0.2250	34549	51072
Diagonals	*DIAG 1*	0.009823	0.0259	0.1775	16636	811
	DIAG 2	0.006510	0.0265	0.1500	8230	561
	DIAG 3	0.004680	0.0210	0.1300	4196	293
	DIAG 4	0.004076	0.0218	0.1100	2769	225
Posts	*POST 1*	0.029408	0.2564	0.2243	84353	37808
	POST 2	0.027096	0.2297	0.2145	80994	11608
	POST 3	0.005848	0.1542	0.0750	234	12753
	POST 4	0.003600	0.0491	0.0750	233	932
Cross-girders	*CGIRD*	0.023284	0.3950	0.0985	1497	173655
Stringers	*STRIN*	0.009600	0.2000	0.0890	968	24316
Bracing elements	*BRAC 1*	0.002122	0.0205	0.0710	188	98
	BRAC 2	0.001061	0.0205	0.0205	49	49

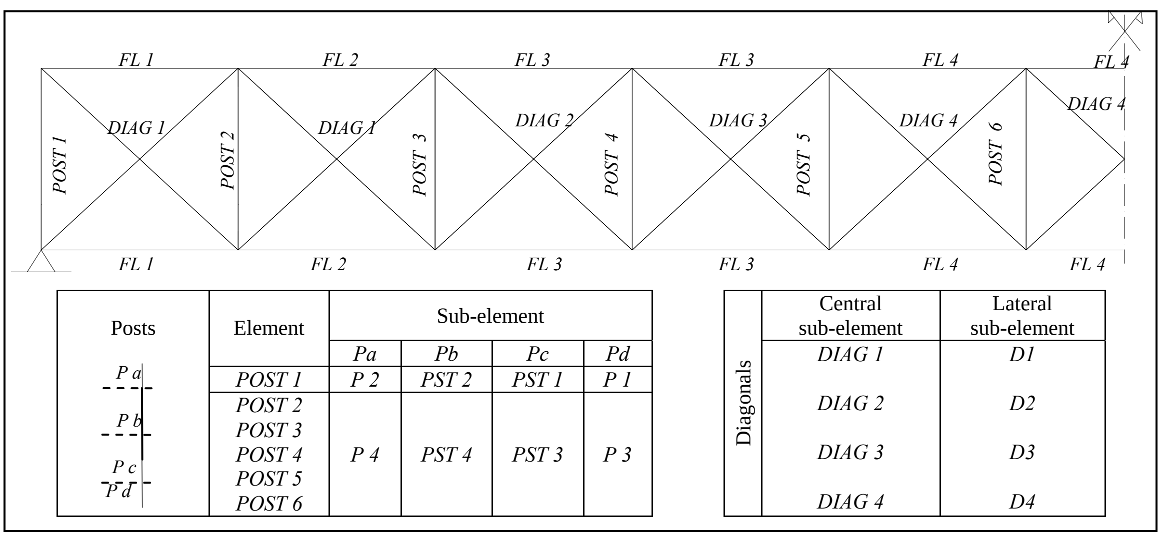

Posts	Element	Sub-element			
		Pa	*Pb*	*Pc*	*Pd*
	POST 1	*P 2*	*PST 2*	*PST 1*	*P 1*
	POST 2 *POST 3* *POST 4* *POST 5* *POST 6*	*P 4*	*PST 4*	*PST 3*	*P 3*

Diagonals	Central sub-element	Lateral sub-element
	DIAG 1	*D1*
	DIAG 2	*D2*
	DIAG 3	*D3*
	DIAG 4	*D4*

Fig. 4. Elements nomenclature: flanges, diagonals and posts.

For the dead loads, the weight of the steel, the weight of the reinforced concrete slab deck, footways and bridge rails were considered. The structure's weight was modeled automatically by the structural analysis software (SAP2000 2003) and was multiplied by 1.1, in order to account for the fastening's weight (gusset's plates, weldings and rivets). The following values were adopted for the material's density: 77 kN/m^3 (steel) and 25 kN/m^3 (reinforced concrete).

In this preliminary analysis, the actions corresponding to the wind and earthquake were not considered. The structure was only submitted to the live loads mentioned in the Portuguese National Standard (RSA 1983) for class I highway bridges:

- Live load of 4 kN/m^2 (Q_{distr}) uniformly distributed over the deck, plus a transversal load of 50 kN/m acting on every possible position of the deck;
- Or, vehicle-type, acting on every possible position of the deck ($Q_{vehicle}$);
- Live load of 3 kN/m^2 uniformly distributed on the footways or concentrated load of 20 kN ($Q_{footway}$) acting on the bridge rails.

In this analysis were considered the following load combinations:

ULTIMATE LIMIT STATES:

$$\textit{ULT 1:}\ \ 1.35 \cdot G + 1.5 \cdot (Q_{vehicle} + Q_{footway}) \tag{1}$$

$$\textit{ULT 2:}\ \ 1.35 \cdot G + 1.5 \cdot (Q_{distr} + Q_{footway}) \tag{2}$$

SERVICEABILITY LIMIT STATES:

$$\textit{SERV 1:}\ \ G + \Psi_1 \cdot (Q_{vehicle} + Q_{footway}) \tag{3}$$

$$\textit{SERV 2:}\ \ G + \Psi_1 \cdot (Q_{distr} + Q_{footway}),\ \ \Psi_1 = 0.4 \text{ (according to RSA 1983)} \tag{4}$$

For each ultimate limit state combination, were considered different positions for the loads applied, namely:

- For *ULT 1* were considered four different positions for the normalized vehicle-type;
- For *ULT 2* were considered two positions for the transversal load (Q_{distr} = 50 kN/m).

For the serviceability limit state combinations, *SERV 1* and *SERV 2*, the vehicle-type and transversal load were located in the mid-span, which corresponds to the maximum deflection. For the vehicle-type combination (*SERV 1*), two different loading cases were considered:

- Vehicle-type centered in the bridge’s cross-section (*SERV 1-A*);
- Vehicle-type with maximum eccentricity in the bridge’s cross-section (*SERV 1-B*).

2.2 Analysis methodology

As stated in section 2.1, each diagonal and post were divided into three sub-elements, where the lateral sub-elements represent the joint's length. The objective of this study was to evaluate the influence of the joint's stiffness in the structural response. Thus, in this analysis, the axial stiffness of those sub-elements, $EA_{NL,}$ was varied in the range [0.5*EA*; 1.5*EA*] and for the central sub-element it was used the nominal axial stiffness, *EA*. The structural response was evaluated for the following values: 0.5*EA*, 0.6*EA*, 0.7*EA*, 0.8*EA*, 0.9*EA*, 1.0*EA*, 1.1*EA*, 1.2*EA*, 1.3*EA*, 1.4*EA* e 1.5*EA*. For each case, the maximum mid-span deflection, the maximum axial forces and corresponding maximum stress in the bars (diagonals, posts, upper and bottom flanges) and the structural natural frequencies, were analyzed.

2.3 Numerical results

The maximum axial forces and corresponding maximum stresses analysis was made for the ultimate limit state combinations. In Table 3 are presented the maximum axial forces, N_{max}, and corresponding maximum stresses, σ_{max}, calculated for each axial stiffness value, EA_{NL}.

Table 3 – Maximum axial force and stress: diagonals, posts and flanges

	Diagonal		Post		Upper flange		Bottom flange	
EA_{NL}/EA	N_{max} (kN)	σ_{max} (MPa)	N_{max} (kN)	σ_{max} (MPa)	N_{max} (kN)	σ_{max} (MPa)	N_{max} (kN)	σ_{max} (MPa)
0.5	-855.44	-174.17	-690.13	-46.93	-3401.44	-131.99	3300.13	128.06
0.6	-854.95	-145.06	-690.79	-39.15	-3406.27	-132.18	3302.16	128.14
0.7	-854.52	-124.27	-691.32	-33.58	-3409.84	-132.32	3303.80	128.20
0.8	-854.15	-108.69	-691.75	-29.40	-3412.59	-132.42	3305.00	128.25
0.9	-853.83	-96.58	-692.11	-26.15	-3414.77	-132.51	3305.90	128.28
1	**-853.56**	**-86.89**	**-692.42**	**-23.55**	**-3416.55**	**-132.58**	**3306.61**	**128.31**
1.1	-853.31	-78.97	-692.68	-21.41	-3418.02	-132.64	3307.17	128.33
1.2	-853.10	-72.37	-692.90	-19.63	-3419.27	-132.68	3307.63	128.35
1.3	-852.92	-66.79	-693.10	-18.13	-3420.33	-132.73	3308.01	128.37
1.4	-852.75	-62.01	-693.27	-16.84	-3421.26	-132.76	3308.33	128.38
1.5	-852.60	-57.86	-693.42	-15.72	-3422.06	-132.79	3308.60	128.39

Fig. 5 illustrates the location of the elements with maximum stress.

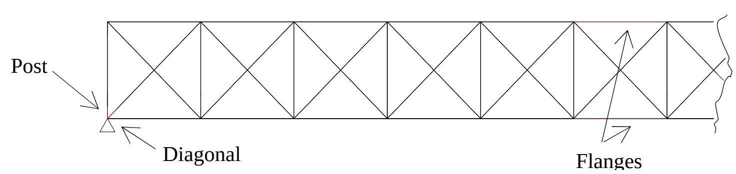

Fig. 5. Elements with maximum stress.

The maximum stress surges at the diagonal for EA_{NL}/EA = 0.5, and corresponds to 174.17 MPa. Consequently, for the analysis performed in this study and not considering the instability at the local or global level, the structural safety (REAE 1986) was verified.

$$\sigma_{máx} = 174.17\,\text{MPa} < f_{yd} = \frac{f_{yk}}{1.1} = \frac{225}{1.1} = 204.55\,\text{MPa} \tag{5}$$

Fig. 6 represents the evolution of the maximum axial force at the diagonals, posts, upper and bottom flanges, in function of the EA_{NL} value.

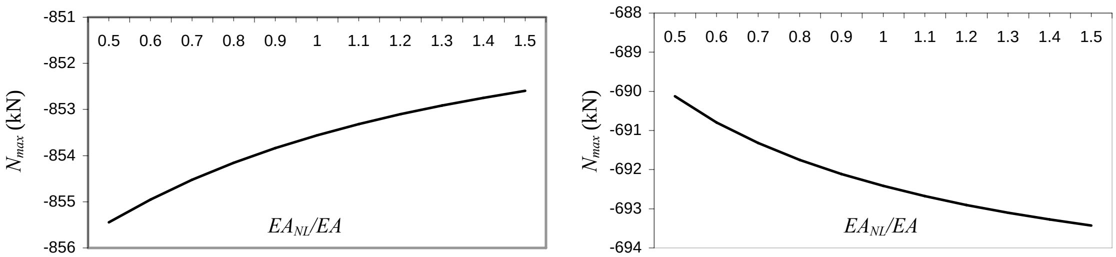

(a) Diagonal (b) Post

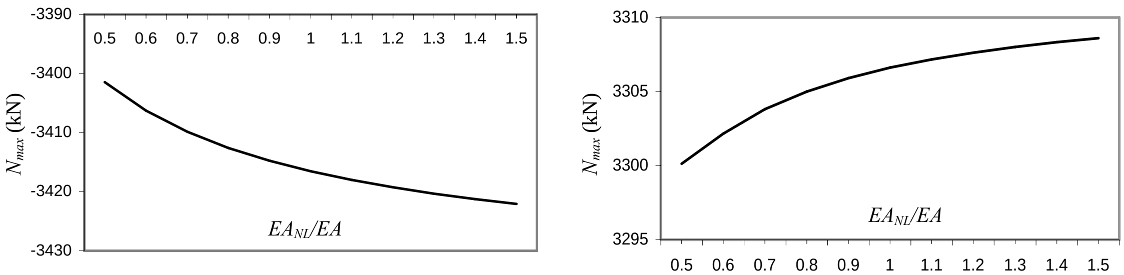

(c) Upper flange (d) Bottom flange

Fig. 6. Maximum axial forces, function of the axial stiffness.

The maximum deflection was analyzed for the serviceability limit state combinations, *SERV 1-A, SERV 1-B* e *SERV 2*. The combination *SERV 2* gives the maximum values. Table 4 and Fig. 7 give the result of the analysis in tend of maximum mid-span deflection.

Table 4 – Maximum mid-span deflection

EA_{NL}/EA	$\delta_{1/2span}$ (cm)		
	SERV 1-A	*SERV 1-B*	*SERV 2*
0.5	4.38	4.26	4.42
0.6	4.32	4.20	4.35
0.7	4.28	4.16	4.31
0.8	4.25	4.12	4.28
0.9	4.22	4.10	4.25
1	4.20	4.08	4.23
1.1	4.18	4.06	4.21
1.2	4.17	4.05	4.20
1.3	4.16	4.04	4.19
1.4	4.15	4.02	4.18
1.5	4.14	4.02	4.17

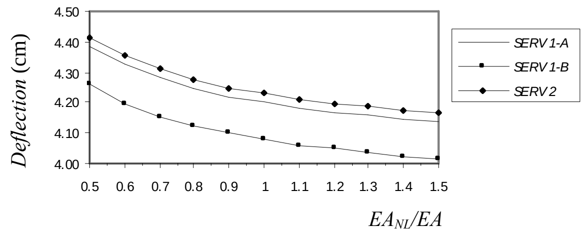

Fig. 7. Mid-span deflection, function of the axial stiffness.

In Table 5 are presented the first 16 vibration modes and natural frequencies of the structure, calculated by the structural analysis software (SAP2000 2003).

Table 5 – Natural frequencies and vibration modes

Vibration modes			Frequencies f (Hz)
1	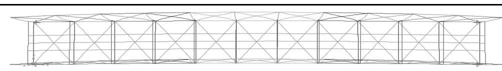 XOY	Transversal bending of the overall structure	2.12
2	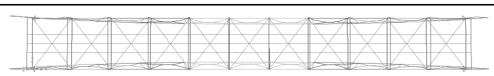 XOY	Transversal bending of the main girders	2.97
3 a 13	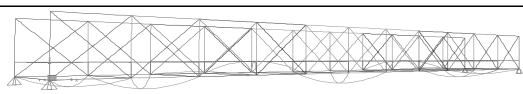 3D	Local bending of the bracing elements	3.03
14	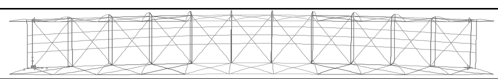 XOY	Transversal bending of the overall structure	3.90
15	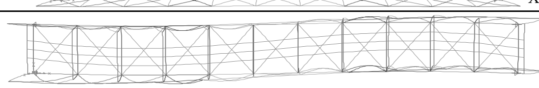 XOY	Transversal bending of the overall structure	5.03
16	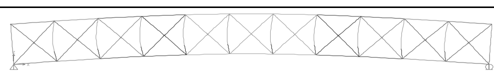 XOZ	In-plane bending of the overall structure	5.18

3. CONCLUSIONS

The maximum deflection was increased 4% for EA_{NL}/EA = 0.5. For this stiffness reduction factor, the axial forces and corresponding stress in the structural elements have the following variations:

- Diagonals: the maximum axial force increased by 0.2% and the corresponding stress increased by 50%.
- Posts: the maximum axial force reduced by 0.3% and the corresponding stress increased by 50%.
- Upper flanges: the maximum axial force and corresponding stress reduced by 0.4%.
- Bottom flanges: the maximum axial force and corresponding stress reduced by 0.2%.

The reasons for these small variations, in terms of axial forces and mid-span deflection, can be pointed out. First, the structure's behavior is essentially isostatic. In spite the presence of two diagonals at each panel, its stiffness is significantly inferior than the flange's stiffness. Consequently, the loads distribution within the structure practically does not depend of the elements stiffness. Secondly, only diagonals and posts were divided in 3 sub-elements and the length of the lateral sub-element represents a small percentage of the total element's length (26% for the diagonals and 20% for the posts).

The first two vibration modes corresponding to global bending of the overall structure have the natural frequencies of 2.12 Hz and 2.97 Hz. From the third to the thirteen vibration modes, the natural frequency is 3.03 Hz and the vibration modes correspond to local bending of the bracing elements.

The joint's stiffness of the bridge S. João de Loure has a significant influence in its structural response, mainly in terms of stress. The axial forces don't vary in a significant way with the joint's stiffness variation. But, as expected, when the cross-section's area of the elements is reduced in 50%, the corresponding stress is increased by the same proportion. However, as verified by the present analysis, the safety coefficient used in the bridge's design is probably sufficient to cover the variations in the axial stiffness caused by deterioration due to, e.g. corrosion (Brinckerhoff 1993). In this way, the axial stiffness variation induced by a non exaggerated cross-section's area variation won't put at risk the bridge structural safety.

REFERENCES

Brinckerhoff, P., “Bridge Inspection and Rehabilitation”, Ed. Louis G. Silano, P.E. ISBN 0-471-53262-2, 1993.

Fernandes, C. and Silva, H., “Bridge's evaluation, maintenance and strengthening”, Civil Engineering Department, University of Aveiro, Aveiro, Portugal, 2004 (in portuguese).

Freire, P. C. M.; Martins, M. R. F. and Torres, M. T. P.,“Steel highway bridges”, Junta Autónoma de Estradas, 1998 (in portuguese).

Furtado, A. C. and Marques, A., “Maintenance and rehabilitation assessment of the S. João de Loure bridge –Vouga's river”, Civil Engineering Department, University of Aveiro, Aveiro, Portugal, 2003 (in portuguese).

RSA – Regulamento de Segurança e Acções para Estruturas de Edifícios e Pontes, Decreto de Lei nº 235/83, 31 May, 1983 (in portuguese).

REAE – Regulamento de Estruturas de Aço para Edifícios, Decreto de Lei nº 211/86, 31 July, 1986 (in portuguese).

S. João de Loure bridge – Drawings (AutoCAD format), 2001.

SAP2000 Nonlinear 8.15, Computer and Structures, Inc., 2003.

Varum, H., “Seismic assessment, strengthening and repair of existing buildings”; PhD Thesis - University of Aveiro, Aveiro, Portugal, 2003.